



HAL
open science

PHA-Based Feedback Control of a Biomimetic AUV for Diver Following: Design, Simulations and Real-Time Experiments

Mart Ratas, Ahmed Chemori, Maarja Kruusmaa

► **To cite this version:**

Mart Ratas, Ahmed Chemori, Maarja Kruusmaa. PHA-Based Feedback Control of a Biomimetic AUV for Diver Following: Design, Simulations and Real-Time Experiments. ECC 2022 - European Control Conference, Jul 2022, London, United Kingdom. pp.503-509, 10.23919/ECC55457.2022.9838054 . lirmm-03720185

HAL Id: lirmm-03720185

<https://hal-lirmm.ccsd.cnrs.fr/lirmm-03720185>

Submitted on 11 Jul 2022

HAL is a multi-disciplinary open access archive for the deposit and dissemination of scientific research documents, whether they are published or not. The documents may come from teaching and research institutions in France or abroad, or from public or private research centers.

L'archive ouverte pluridisciplinaire **HAL**, est destinée au dépôt et à la diffusion de documents scientifiques de niveau recherche, publiés ou non, émanant des établissements d'enseignement et de recherche français ou étrangers, des laboratoires publics ou privés.

PHA-Based Feedback Control of a Biomimetic AUV for Diver Following: Design, Simulations and Real-Time Experiments

Mart Ratas¹, Ahmed Chemori² and Maarja Kruusmaa¹

Abstract—This paper deals with the use of a passive hydrophone array (PHA) for following non-stationary underwater objects with a miniature biomimetic autonomous underwater vehicle. Current acoustic underwater localization systems are large and expensive. They are not well suited for using on miniature, low-cost underwater vehicles. However, compact size and low cost are necessary when developing autonomous vehicles that can be widely used by recreational and professional divers. As an alternative, a simple hydrophone array is developed for a biomimetic 4-flipper U-CAT AUV (Autonomous Underwater Vehicle). The array is used to measure the bearing of a single acoustic beacon. Two control approaches are proposed for navigating the vehicle towards the beacon. The whole system is validated both in a simulator and in a natural environment using two scenarios: 1) navigating towards a stationary beacon and 2) navigating towards a beacon mounted on a diver. The results show that the proposed control system is a viable approach to be used for diver following.

I. INTRODUCTION

The number of robots used in everyday life is rapidly growing. An important factor that enables this growth is the increasing availability of low-cost robotic tools and technologies [1]–[4]. Mobile mass-produced robots, such as lawnmowers, vacuum cleaners and package delivery vehicles use technologies that are affordable to every robotics enthusiast. However, this is only true in the terrestrial and aerial domain. The availability of low-cost solutions in the underwater domain drops rapidly which in turn restricts the development of widely exploited underwater robotic tools.

The problem becomes apparent in the field of underwater localization. Due to physical properties of the water the localization is mostly limited to using the combination of acoustic, inertial or magnetic devices. Dead reckoning using inertial and magnetic devices is a widely available technology and finds a lot of use in underwater robotics [5], but it usually does not offer sufficient accuracy without the use of high-cost doppler velocity logs [6] or acoustic doppler current profilers [7]. The system gets even more complex when relative navigation with respect to stationary or moving objects is desired. Most traditional relative acoustic methods such as ultra-short baseline (USBL) and long baseline (LBL) can provide high positioning accuracy, but they are also expensive. The same goes with the imaging sonars which are often used for feature recognition and SLAM [8]. In addition to the high price, most of the acoustic devices,

even the simplest echo sounders, are usually large devices not suitable for miniature vehicles. Few studies have been conducted to develop simpler, lower cost and small-size localization methods. One alternative is to use visual methods such as visual SLAM [9] and visual velocity log [10]. Recent development of chip scale atomic clocks has also provided a possibility to develop simpler acoustic range measurement systems [11], [12]. Localization using a single beacon range measurement is analysed in [13].

One of the simplest acoustic localization systems is based on beamforming of hydrophone array signals to passively identify the bearing of a transmitting beacon. Acoustic beamforming has been thoroughly studied and it is used in many terrestrial [14] and underwater applications [15]. However, as it provides much less useful localization information compared to more advanced acoustic systems, it finds very limited use in the control of autonomous underwater vehicles. Localization of a vehicle using only a bearing information from a single transmitter is demonstrated in [16]. However, they have acquired the data using high-precision USBL device omitting the range measurements.

This paper shows that beamforming with an hydrophone array is a viable alternative to be used in the control of an underwater robot in certain situations. It demonstrates a control of a miniature, biomimetic U-CAT AUV [17] using a simple custom-made beamforming system. We propose control approaches for localizing and navigating towards steady or moving transmitters. We validate the beamforming system and the control approaches in a scenario of real-time diver tracking and following. Diver tracking is tested both in simulations and in natural environment experiments.

Diver tracking [18] is necessary for developing robotic tools that can work in collaboration with divers during critical underwater missions, with an aim to increase diver safety and efficiency. Diver following has previously been studied using different methods. Tracking of a diver from an autonomous surface vehicle using traditional USBL system is described in [19]. Besides, a visual method based on the so called curiosity algorithm is proposed in [20]. Recently, the control for a diver following based on visual and acoustic signals data fusion measured by low-cost sensors is addressed in [18].

The rest of the paper is organized as follows. Section II gives an overview of the U-CAT vehicle and section III describes the hydrophone array system and its characterization. Section IV describes the control of the U-CAT based the hydrophone array readings. The system is validated through numerical simulations in section V and real-time experiments

¹Mart Ratas and Maarja Kruusmaa are with Centre for Biorobotics, Tallinn University of Technology, Tallinn, Estonia, mart.ratas@ttu.ee

²Ahmed Chemori is with LIRMM, University of Montpellier, CNRS, Montpellier, FRANCE. Email: Ahmed.Chemori@lirmm.fr

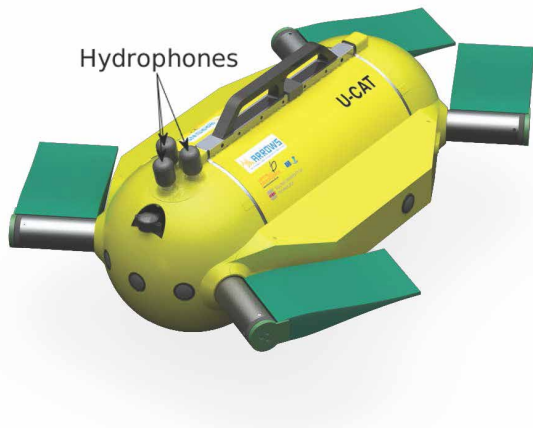


Fig. 1. View of the passive hydrophone array (PHA) on U-CAT biomimetic AUV.

in section VI.

II. U-CAT BIOMIMETIC AUV

Beamforming and diver tracking system was implemented and tested on a biomimetic U-CAT AUV [21]–[23]. U-CAT is an experimental biomimetic underwater vehicle propelled by 4 oscillating fins. It was developed in the framework of European Commission funded research project ARROWS [24] for autonomous and semi-autonomous inspection of confined areas, such as shipwrecks, caves and man-made underwater structures. Fin-based locomotion is studied on U-CAT to identify its advantages with respect to conventional propeller-driven designs. The main advantages are believed to be high maneuverability, small sediment disturbance and smaller risk of getting tangled. In addition, fin-based locomotion is much safer for the surrounding environment than propellers. Soft fins can be safely operated in the vicinity of divers without any threat to the vehicle or to divers themselves. Taking also into account the small size of the vehicle, U-CAT is a good platform for studying diver-robot cooperation.

U-CAT can be actuated in all the 6 degrees of freedom. It is small compared to most of the traditional autonomous robots, having the length of 56 cm and weight of 19 kg. Fins are actuated by 60 W brushless DC motors and the power is provided by internal batteries allowing at least 6 hours of autonomy.

Like other vehicles (e.g. Leonard [25]) U-CAT is equipped with only low-cost sensors. It uses an Applicon acoustic modem for underwater communication and range measurements, two active buoyancy control modules, a custom-made echo sounder array for close-distance obstacle avoidance and Point Grey Chameleon camera as the main payload sensor. However, this is not used within the context of this paper. Depth is measured using GEMS 3101 analog output processor sensor with 18-bit DAQ. The attitude of the vehicle is measured using Invensense MPU-6050 IMU. The depth sampling frequency is 10 Hz and the IMU sampling frequency is 5 Hz. The control of the vehicle is running

on the on-board computer which has an ARM Cortex A9 quad-core 1 GHz processor. The software is developed using ROS middleware [26]. A detailed description of the control architecture is presented in [23]. The rigid body dynamics of the U-CAT is modeled in 6 degrees of freedom using the standard Fossen’s vectorial model of marine craft [27]

$$\begin{aligned} \dot{\eta} &= \mathbf{J}(\eta)\boldsymbol{\nu} \\ \mathbf{M}\dot{\boldsymbol{\nu}} + \mathbf{C}(\boldsymbol{\nu})\boldsymbol{\nu} + \mathbf{D}(\boldsymbol{\nu})\boldsymbol{\nu} + \mathbf{g}(\eta) &= \boldsymbol{\tau} \end{aligned} \quad (1)$$

where $\boldsymbol{\eta} = [x, y, z, \varphi, \theta, \psi]^T$ is the vector of positions in the earth-fixed frame, $\boldsymbol{\nu} = [u, v, w, p, q, r]^T$ is the vector of velocities in the body-fixed frame and $\mathbf{J}(\boldsymbol{\eta}) \in \mathbb{R}^{6 \times 6}$ is the transformation matrix mapping from the body-fixed frame to the earth-fixed frame. \mathbf{M} is the system inertia matrix including added mass, $\mathbf{C}(\boldsymbol{\nu})$ is the Coriolis-centripetal matrix, $\mathbf{D}(\boldsymbol{\nu})$ is the damping matrix, $\mathbf{g}(\boldsymbol{\eta})$ is the vector of gravitational/buoyancy forces and moments and $\boldsymbol{\tau}$ is the vector of control inputs. The vector $\boldsymbol{\tau}$ of control inputs is a combination of thrust forces of each fin. The thrust forces have previously been experimentally identified depending on the oscillation amplitude, frequency and the oscillation offset. The model parameters \mathbf{M} , $\mathbf{C}(\boldsymbol{\nu})$, $\mathbf{D}(\boldsymbol{\nu})$ and $\mathbf{g}(\boldsymbol{\eta})$ have been found using theoretical calculations and experimental identification methods [17] [28].

III. PASSIVE HYDROPHONE ARRAY (PHA)

A low-cost array of 3 Aquarian Audio H1c hydrophones is used for establishing the heading relative to the beacon.

Sonotronics EMT-01-3 Equipment Marker Transmitter operating at 9.6kHz is used as the beacon. The beacon transmits a short burst signal every one second. The signal is received by each hydrophone and is amplified and filtered using a second order filter on a custom board. The signals are then digitized using a 16 bit analog digital converter with the sampling frequency of 200 kHz. Digitized signals are processed using a dedicated BeagleBone Black single-board computer.

The hydrophone array is positioned on top of the robot in the fore. The array is tilted 14 degrees towards the fore of the vehicle to improve the reception from the front. The hydrophones in the array are positioned in a tight pattern of an equilateral triangle as seen in Fig. 1. As it is necessary to have a direct line of sight from each hydrophone to the beacon, this kind of a configuration allows to listen only to beacons above and in front of the vehicle, but not below. While a greater number of hydrophones could remove this limitation, it was considered that the additional cost outweighed the benefit. This was considered when developing and testing the control.

The incoming signal is compared to a threshold and 10 ms of signal is extracted starting from the time when the threshold was exceeded. The extracted signal is digitally filtered around the beacon transmitting frequency. A typical example of raw and filtered data with the threshold can be seen in Fig. 2. The phases of each signal are obtained using the phase of the Fourier coefficient corresponding to

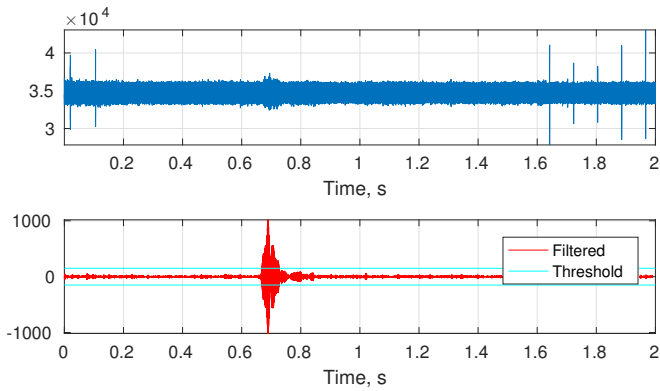


Fig. 2. Raw signal (up) and signal filtered around 9.6kHz along the threshold (down).

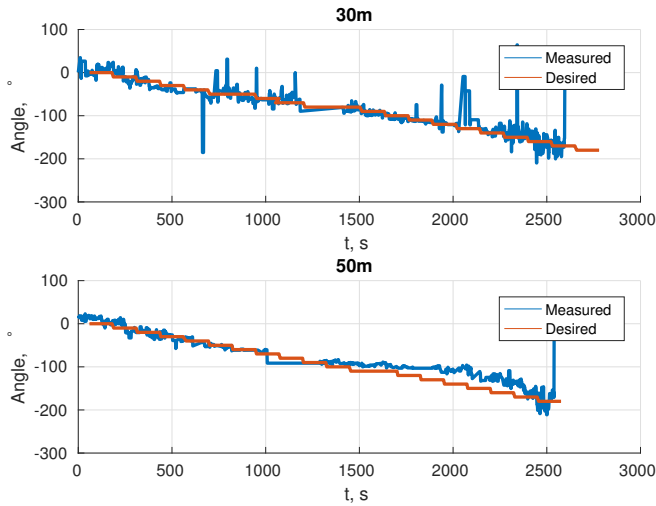


Fig. 3. Passive hydrophone array (PHA) characterization at 30m (up) and 50m (down): the measured angle and the desired angle.

the required frequency. The differences in phase for each hydrophone are then used to first find the angle of approach for a pair of hydrophones and then to find the direction of arrival of the signal making use of the far field assumption (arriving signals are assumed to be parallel). A unit vector pointing towards the estimation of the beacon position with respect to the hydrophone array orientation is produced. The orientation is transformed into a world fixed coordinate frame using the attitude and the orientation of the vehicle. Since the computation on the BeagleBone Black can take some time, a buffer of the robot's IMU is kept to make sure that the received relative direction is rotated using the robot's orientation at the time when the signal was actually received. Since there can be many obstacles underwater that can reflect or otherwise disturb the signal, signals with undesirable characteristics can sometimes be observed. These signals are discarded automatically.

A. System characterization

Experiments were carried out in sheltered waters to identify the hydrophone system's performance in a natural environment. Performance was estimated by comparing the

bearing measurements of the hydrophone array to the actual beacon bearing. During the experiments U-CAT was fixed on a mechanism that constrained all its degrees of freedom except yaw. The yaw was set manually by a person. To measure the actual bearing of the beacon the mechanism was equipped with a rotational scale which allowed the orientation of the vehicle to be read. Zero orientation was matched with the zero bearing.

Both the beacon as well as the robot were at a depth of 2 m.

The distance between the two was 20, 30, 40 and 50 m in various experiments. In these experiments the robot was not actuated but was moved manually. In each experiment, the robot started looking towards the beacon and was then turned 180° with an increment of 10° . It was held stationary for 2 minutes at each angle ($0^\circ, 10^\circ, \dots, 170^\circ, 180^\circ$).

Typical results from a distance of 30 and 50 m are shown in Fig. 3. As is evident, there is a relatively good correlation between the measured and desired angle. However, it is clear that at larger angles ($> 90^\circ$) the accuracy diminishes. This is expected since the robot and the beacon are at the same depth and the robot itself can be in the way of the direct line of site to the beacon.

The standard deviation from the desired angle is 20.17° at 30m and 19.85° at 50m. This could be considered rather large, but if we consider that (while homing) the robot would be looking towards the beacon most of the time, we would only need to consider smaller angles. If we look at angles below 45° , we find that the standard deviations drop to 19.01° and 11.54° , respectively. It is hard to tell why the result is so much better from a larger distance, but one possible explanation could be the different position of the beacon. In experiments where the beacon was further away the water below the beacon was deeper and it is possible that there was therefore less reflections to disrupt the received signal.

From these preliminary experiments it can be concluded that the passive hydrophone system works with a satisfactory accuracy.

IV. BEACON TRACKING CONTROL DESIGN

A. Description of the control system

The proposed control system is illustrated through the block diagram of Fig. 4. The basic idea of its main module

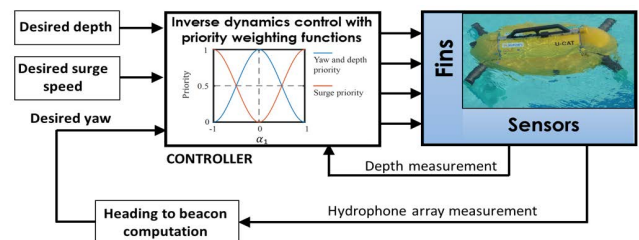


Fig. 4. Block diagram of the proposed control system.

(i.e. CONTROLLER block in Fig. 4) includes an inverse

dynamics controller (also called *state feedback linearization* [27]), and priority weighting functions [28].

The main idea of the state feedback linearization controller consists in exactly linearizing the robot's dynamics with a nonlinear state feedback law. Like other model-based controllers [29] for biomimetic robots, this control scheme has been used in underwater robotics [30] and also for some biomimetic underwater vehicles. In our study, this method is designed by state feedback linearization with acceleration feedforward [27]. To this end, let us consider the dynamic model (1) as well as the following nonlinear state feedback law:

$$\tau = M\mathbf{a}^b + \mathbf{n}(\nu, \eta) \quad (2)$$

where \mathbf{n} is a nonlinear term expressed by:

$$\mathbf{n}(\nu, \eta) = \mathbf{C}(\nu)\nu + \mathbf{D}(\nu)\nu + \mathbf{g}(\eta) \quad (3)$$

\mathbf{a}^b represents the body frame commanded acceleration, it can be calculated as follows based on the transformation between the body and the earth fixed-frames:

$$\mathbf{a}^b = \mathbf{J}^{-1}(\mathbf{a}^n - \dot{\mathbf{J}}\nu)$$

with $\mathbf{a}^n = \ddot{\eta}_d - K_P\dot{\eta} - K_I \int_0^t \dot{\eta} dt - K_D\dot{\eta}$. η_d and $\dot{\eta}_d$ represent desired trajectory and its acceleration, respectively. If we replace the control input (2) in the dynamics (1), we get:

$$(\mathbf{J}\dot{\nu} + \dot{\mathbf{J}}\nu) = \ddot{\eta}_d - K_P\dot{\eta} - K_I \int_0^t \dot{\eta} dt - K_D\dot{\eta} \quad (4)$$

Let us now consider the time derivative of the kinematics of the vehicle in (1) as follows $\dot{\eta} = \mathbf{J}\nu + \dot{\mathbf{J}}\nu$, together with (4) leads to:

$$\ddot{\eta} + K_D\dot{\eta} + K_P\eta + K_I \int_0^t \dot{\eta} dt = 0 \quad (5)$$

The asymptotic stability of this resulting closed-loop dynamics can be guaranteed with an appropriate choice of the feedback gains K_P, K_I, K_D .

In the proposed control architecture of Fig. 4, different DOFs are controlled simultaneously. However, due to the coupled nature of actuation priority weighting function are considered. Indeed, the control input vector generated by the above state feedback control law is multiplied by a priority vector (whose elements are complementary and vary between 0 and 1). The priorities depend on the control action of a single DOF in the following way. When controlling the three DOFs: depth, yaw and surge, a high priority is assigned to yaw and depth when surge control action is small, and vice versa. The desired depth is specified by the user depending on the depth of the beacon. Since the surge is unmeasurable, it is controlled in open loop, its speed is chosen depending of the desired speed of navigation. The desired yaw angle is chosen using the heading relative to the beacon based on the hydrophone array measurements. This control system can be implemented in two ways depending on the controller. Two navigation controllers are proposed, namely *wait control* and *continuous control*, both of which are described below.

B. First navigation controller: Wait control

In this controller (illustrated in Fig. 5), the depth is controlled continuously, while the yaw and surge are controlled alternatively. In this controller, the vehicle remains stationary while waiting for the desired number of pings. Once the desired yaw is obtained (i.e. when the desired number of pings is reached), the yaw is first corrected, then the surge (because it is unmeasurable) is controlled in open-loop to move towards the beacon.

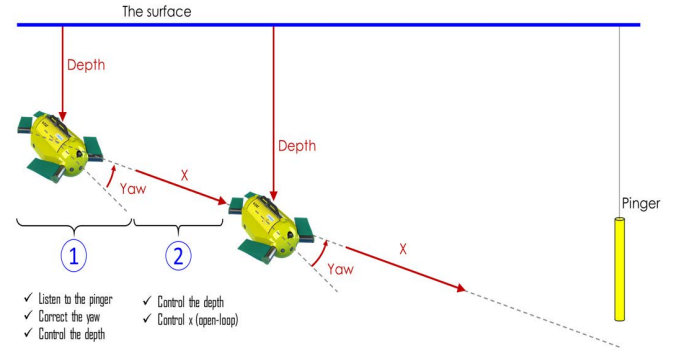


Fig. 5. Illustration of the concept of the wait control.

C. Second navigation controller: continuous control

In the second controller (illustrated in Fig. 6), three DOFs are controlled simultaneously (depth, yaw and surge), where the concept of priority functions is used.

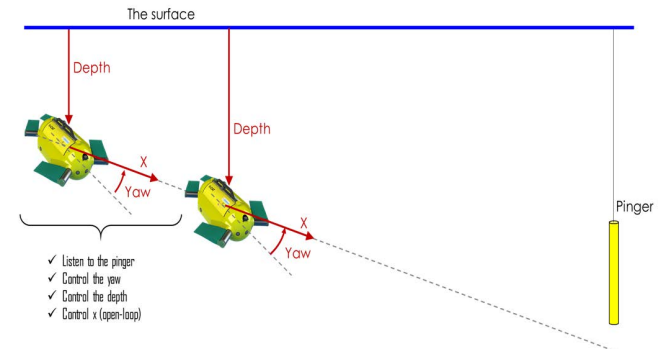


Fig. 6. Illustration of the concept of the continuous control.

V. NUMERICAL SIMULATIONS

Initial verification and comparison of the control approaches was done in simulations. For simulations we used an advantageous feature of Robot Operating System (ROS) that allows seamless switching between the simulated and physical vehicles. It means that the exact code running on the actual robot can be easily tested on the simulated robot. The simulated U-CAT is implemented using the UWSim software [31]. UWSim allows 3D visualization and simulation of the vehicle dynamics and the hardware devices. The dynamics are simulated using UWSim's built in physics engine which

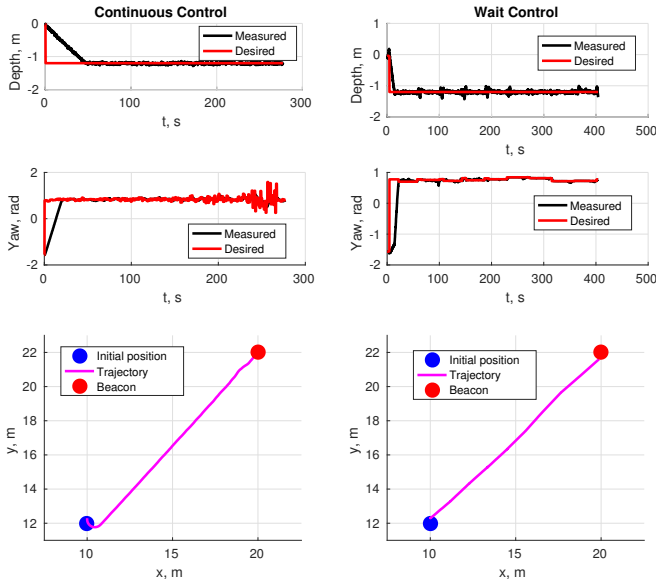


Fig. 7. Depth precision (up), yaw precision (middle) and trajectory (down) for either approach and a stationary beacon.

incorporates the identified U-CAT’s dynamic model [17] [28]. The IMU, depth sensor and hydrophone array are simulated taking into account the actual sampling frequencies, resolutions and noise levels of physical devices. Both proposed control approaches were tested in two scenarios:

- *Homing*: Moving towards a stationary beacon.
- *Diver following*: Following a moving beacon.

A. Homing

First of all it was necessary to show that the robot could locate and reach a stationary beacon. In this simulation, the robot started at a position $x = 10$, $y = 12$, $z = 0$ and had to move towards the beacon at $x = 20$, $y = 22$, $z = -1.2$. At the beginning of the experiment it also had to dive to the beacon depth of $z = -1.2$. The simulation results are shown in Fig. 7. The standard deviation from the desired depth is 0.02 m for continuous control and 0.03 m for wait control. Additionally, the standard deviation from the actual beacon bearing was 3.4° and 6.3° for the two approaches, respectively. The time spent to reach the beacon was 280 s for continuous control and 400 s for the wait control.

It can be seen that both control approaches are able to steer the vehicle to the target. However, the wait control is significantly slower as the vehicle is stationary while waiting for the desired number of pings. Moreover, the results show that wait control generates small oscillations in depth when switching between waiting and surging. The continuous control approach, on the other hand, gets a more noisy desired yaw when getting close to the beacon. The continuous control is also slower at reaching desired depth because in this approach depth, yaw and forward motion are all controlled simultaneously.

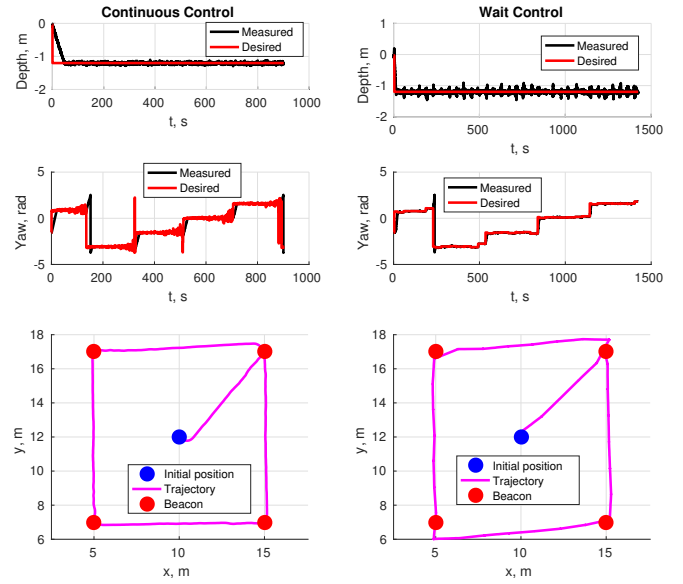


Fig. 8. Depth precision (up), yaw precision (middle) and trajectory (down) for either approach and a moving beacon.

B. Diver following

Both control approaches were also tested in a scenario of a moving beacon. The aim of this scenario is to test if the robot is able to track and reach a beacon at an arbitrary direction. In real conditions this would correspond to the robot tracking a diver who moves to the next position once the robot gets too close. In this scenario, the robot started at the same location as in the previous scenario ($x = 10$, $y = 12$, $z = 0$). The beacon was moved in a rectangular pattern as seen in Figure 8. It was moved to the next location once the robot got closer than 0.5 m from it.

The results for both approaches are shown in Fig. 8. The standard deviation from the desired depth is 0.02 m for continuous control and 0.05 m for wait control. Standard deviation from the actual beacon bearing was 21° and 30° for the two approaches, respectively. The time spent to finish the trajectory following was 900 s for continuous control and 1450 s for the wait control.

The results again show that both approaches are able to control the vehicle to the desired location, however continuous control is more accurate at reaching the beacons and takes less time. There is an overshoot in case of the wait control approach because the robot does not listen to new signals during forward motion. The simulations show that both approaches will get the robot to its intended destination. However, it is clear that the continuous control approach works faster and is more accurate.

VI. REAL-TIME EXPERIMENTAL VALIDATION

The continuous control approach, which showed significantly higher performance in simulations, was also validated in experiments in a natural environment. The experiments were carried out in Rummu Quarry lake in Estonia. The robot was launched from a pier into a water with depth of approximately 4 m. The continuous control approach was

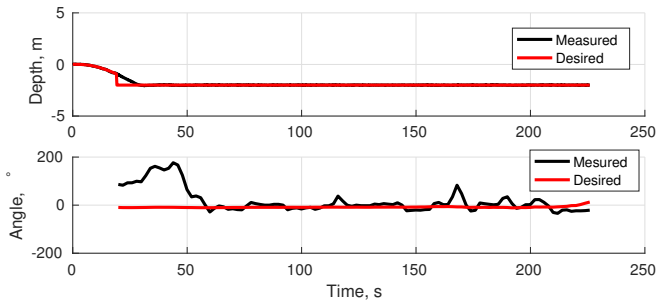


Fig. 9. Moving towards a stationary beacon.

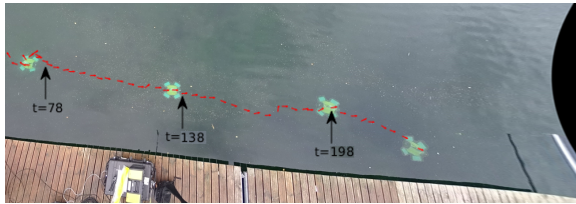


Fig. 10. Trajectory and yaw along with samples in time (in seconds) while moving towards a stationary beacon with the beacon circled in red.

used again to move towards a stationary beacon as well as to follow a moving diver. The vehicle was tethered for safety and for simplified launch and recovery procedures, however it was fully autonomous during experiments.

A. Homing

In this experiment, the beacon was in a fixed position 15 m away from the robot at a depth of 2 m. The robot also dove to a depth of 2 m before starting to track the beacon. The experiment was monitored and the robot was tracked with an super-wide lens overhead camera mounted about 4 m above the testing area.

The resulting depth and yaw tracking for this experiment can be seen in Fig. 9 and the trajectory in Fig. 10. It must be noted that while the depth is measured by the robot, the yaw angle shown in the figure is in fact measured from pictures of the overhead camera. This is because the IMU tends to drift and can thus be unreliable. Because of the considerable lens distortion of the overhead camera, neither the position nor the orientation of the robot could be measured at the very beginning of the experiment which is why the depth measurement starts before the yaw measurement. The standard deviation is 1.4 cm for depth and 20.17° for yaw. The deviation is calculated over the period where the robot had reached the depth of 2 m (from around 40 seconds), as due to the coupled degrees of freedom the vehicle can not precisely control its yaw during full-speed dive. The vehicle reached the target in 225 s.

The results show that the proposed control system is able to steer the vehicle to the desired target while holding depth with high precision. The deviation of yaw is close to the standard deviation of the hydrophone array itself (20.17° at 50 m), showing that the main source of error is the hydrophone array's measurement, not the controller's ability to keep the measured orientation.

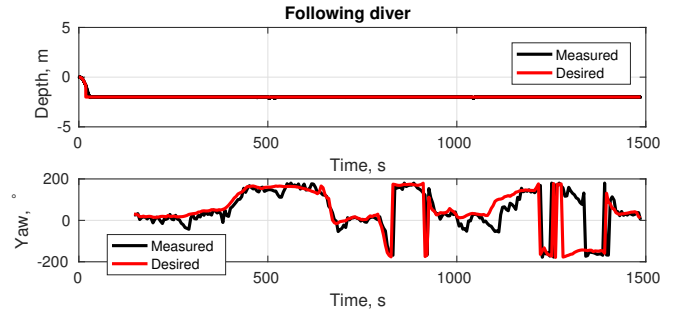


Fig. 11. Trajectory when following a diver.

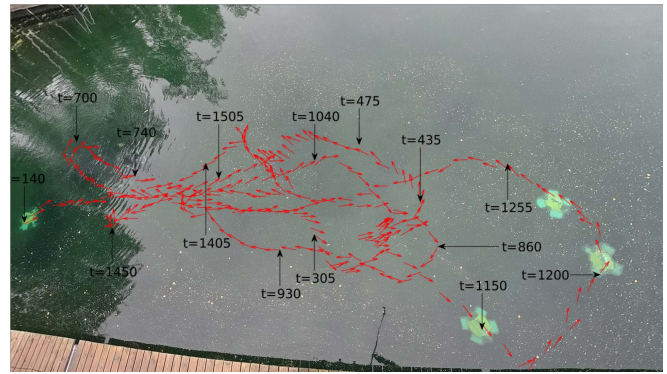


Fig. 12. Trajectory and yaw along with some samples in time (in seconds) while following the diver.

B. Diver following

The next experiment was carried out to identify if the robot can track the beacon at an arbitrary angle in a longer time frame. In order to do this, the beacon was attached to a diver who was instructed to move to different positions under water when the robot gets close. Because moving underwater is not a precise operation for a diver, no clear pattern was set for the diver. The diver was at a rough depth of 2 m. The same depth was set for the robot. As with the last experiment an overhead camera was used to observe the real position of the robot and the diver.

Fig. 11 shows the depth and yaw tracking while Fig. 12 shows the trajectory for this experiment. Again, desired and actual yaw angles were measured from the overhead camera. While it is clear that depth tracking is not a problem with a standard deviation of only 1.8 cm, deviation from desired yaw is a little larger with the standard deviation of 36.7° . Some of that increase likely comes from the fact that the diver moves faster than the robot can listen and react at times but also from engine noise which can not always be completely filtered out.

This experiment shows that the robot had generally no problem following a moving target regardless of the direction of the target. The deviation from desired angle is bigger than in case of a stationary beacon, but that is expected as it is more difficult to locate and follow a moving target. While it can take some time for the robot to orient itself towards the beacon, it always managed to do so and reach the destination at the beacon.

VII. CONCLUSION AND FUTURE WORK

This study shows that a relatively simple and low cost passive hydrophone array (PHA) is a viable option for diver following on a compact underwater robot such as U-CAT. The passive array was shown to have a satisfactory precision in preliminary experiments. Two different control approaches were tested in simulations and the continuous control approach was shown to be superior to the wait control approach. The navigation precision expectedly diminished somewhat in experimental conditions, however it was shown that the main source of error was the passive hydrophone system and not the controller. The robot was easily controlled using the bearing of a beacon, it could hold its depth very well and steer towards the beacon at arbitrary angles.

As a next step, multiple independent beacons could be deployed at the same time for finer localization. Prior knowledge of the world fixed coordinates of the beacons would allow localizing the robot fully. This is one of the goals of the passive hydrophone system described in this study.

VIII. ACKNOWLEDGMENT

This research has received funding from Estonian-French joint collaboration project PHC-PARROT. The authors would like to thank Jaan Rebane as well as other students and Engineers of Centre for Biorobotics who helped develop the U-CAT vehicle and the passive hydrophone system in particular.

REFERENCES

- [1] D. Maalouf, A. Chemori, and V. Creuze, "Stability analysis of a new extended l1 controller with experimental validation on an underwater vehicle," in *52nd IEEE Conference on Decision and Control*, 2013, pp. 6149–6155.
- [2] J. Guerrero, J. Torres, V. Creuze, and A. Chemori, "Observation-based nonlinear proportional-derivative control for robust trajectory tracking for autonomous underwater vehicles," *IEEE Journal of Oceanic Engineering*, vol. 45, no. 4, pp. 1190–1202, 2019.
- [3] A. Tijjani, A. Chemori, and V. Creuze, "Robust adaptive tracking control of underwater vehicles: Design, stability analysis, and experiments," *IEEE/ASME Transactions on Mechatronics*, vol. 26, no. 2, pp. 897–907, 2021.
- [4] E. Campos, J. Monroy, H. Abundis, A. Chemori, V. Creuze, and J. Torres, "A nonlinear controller based on saturation functions with variable parameters to stabilize an auv," *International Journal of Naval Architecture and Ocean Engineering*, vol. 11, no. 1, pp. 211–224, 2019.
- [5] L. Whitcomb, D. Yoerger, and H. Singh, "Advances in doppler-based navigation of underwater robotic vehicles," in *Robotics and Automation, 1999. Proceedings. 1999 IEEE International Conference on*, vol. 1, 1999, pp. 399–406 vol.1.
- [6] M. Karimi, M. Bozorg, and A. R. Khayatian, "A comparison of dvl/ins fusion by ukf and ekf to localize an autonomous underwater vehicle," in *Robotics and Mechatronics (ICRoM), 2013 First RSI/ISM International Conference on*, Feb 2013, pp. 62–67.
- [7] L. Medagoda, J. C. Kinsey, and M. Eilders, "Autonomous underwater vehicle localization in a spatiotemporally varying water current field," in *2015 IEEE International Conference on Robotics and Automation (ICRA)*, May 2015, pp. 565–572.
- [8] A. Mallios, P. Ridaou, D. Ribas, F. Maurelli, and Y. Petillot, "EKF-slam for auv navigation under probabilistic sonar scan-matching," in *Intelligent Robots and Systems (IROS), 2010 IEEE/RSJ International Conference on*, Oct 2010, pp. 4404–4411.
- [9] A. Kim and R. M. Eustice, "Real-time visual slam for autonomous underwater hull inspection using visual saliency," *IEEE Transactions on Robotics*, vol. 29, no. 3, pp. 719–733, June 2013.
- [10] J. Salvi, Y. Petillo, S. Thomas, and J. Aulinas, "Visual slam for underwater vehicles using video velocity log and natural landmarks," in *OCEANS 2008*, Sept 2008, pp. 1–6.
- [11] S. E. Freeman, L. Emokpae, and G. F. Edelmann, "Wireless underwater acoustic beamforming using chip-scale atomic clock timers," *The Journal of the Acoustical Society of America*, vol. 138, no. 3, pp. 1948–1948, 2015.
- [12] E. Fischell, T. Schneider, and H. Schmidt, "Design, implementation, and characterization of precision timing for bistatic acoustic data acquisition," *IEEE Journal of Oceanic Engineering*, vol. 41, no. 3, pp. 583–591, July 2016.
- [13] S. Wang, L. Chen, H. Hu, and D. Gu, "Single beacon based localization of auvs using moving horizon estimation," in *2013 IEEE/RSJ International Conference on Intelligent Robots and Systems*, Nov 2013, pp. 885–890.
- [14] J. M. Valin, F. Michaud, J. Rouat, and D. Letourneau, "Robust sound source localization using a microphone array on a mobile robot," in *Intelligent Robots and Systems, 2003. (IROS 2003). Proceedings. 2003 IEEE/RSJ International Conference on*, vol. 2, Oct 2003, pp. 1228–1233 vol.2.
- [15] X. Lurton, *An introduction to underwater acoustics: principles and applications*. Springer Science & Business Media, 2002.
- [16] C. Becker, D. Ribas, and P. Ridaou, "Simultaneous sonar beacon localization & auv navigation," *IFAC Proceedings Volumes*, vol. 45, no. 27, pp. 200–205, 2012.
- [17] W. Remmas, A. Chemori, and M. Kruusmaa, "Inverse-model intelligent control of fin-actuated underwater robots based on drag force propulsion," *Ocean Engineering*, vol. 239, no. 1, p. 109883, 2021.
- [18] —, "Diver tracking in open waters: A low-cost approach based on visual and acoustic sensor fusion," *Journal of Field Robotics*, vol. 38, no. 3, pp. 494–508, 2021.
- [19] N. Mišković, N. Stilinović, Z. Vukić *et al.*, "Guidance and control of an overactuated autonomous surface platform for diver tracking," in *Control & Automation (MED), 2013 21st Mediterranean Conference on*. IEEE, 2013, pp. 1280–1285.
- [20] Y. Girdhar and G. Dudek, "Exploring underwater environments with curiosity," in *Computer and Robot Vision (CRV), 2014 Canadian Conference on*. IEEE, 2014, pp. 104–110.
- [21] T. Salumäe, R. Raag, J. Rebane, A. Ernits, G. Toming, M. Ratas, and M. Kruusmaa, "Design principle of a biomimetic underwater robot u-cat," in *Oceans-St. John's, 2014*. IEEE, 2014, pp. 1–5.
- [22] A. Chemori, K. Kuusmik, T. Salumäe, and M. Kruusmaa, "Depth control of the biomimetic u-cat turtle-like auv with experiments in real operating conditions," in *Robotics and Automation (ICRA), 2016 IEEE International Conference on*. Stockholm, Sweden: IEEE, May 2016, pp. 1–6.
- [23] T. Salumäe, A. Chemori, and M. Kruusmaa, "Motion control architecture of a 4-fin u-cat auv using dof prioritization," in *Intelligent Robots and Systems (IROS 2016), 2016 IEEE/RSJ International Conference on*. IEEE, 2016.
- [24] (2016) Fp7 arrows project website. [Online]. Available: <http://www.arrowsproject.eu/>
- [25] J. Guerrero, J. Torres, V. Creuze, and A. Chemori, "Adaptive disturbance observer for trajectory tracking control of underwater vehicles," *Oceanic Engineering*, vol. 200, p. 107080, 2020.
- [26] M. Quigley, K. Conley, B. Gerkey, J. Faust, T. Foote, J. Leibs, R. Wheeler, and A. Y. Ng, "Ros: an open-source robot operating system," in *ICRA workshop on open source software*, vol. 3, no. 3.2. Kobe, Japan, 2009, p. 5.
- [27] T. I. Fossen, *Handbook of marine craft hydrodynamics and motion control*. John Wiley & Sons, 2011.
- [28] T. Salumäe, A. Chemori, and M. Kruusmaa, "Motion control of a hovering biomimetic 4-fin underwater robot," *IEEE Journal of Oceanic Engineering*, vol. 44, no. 1, pp. 54–71, 2019.
- [29] N. Carlesi and A. Chemori, "Nonlinear model predictive running control of kangaroo robot: A one-leg planar underactuated hopping robot," in *2010 IEEE/RSJ International Conference on Intelligent Robots and Systems*, 2010, pp. 3634–3639.
- [30] D. Maalouf, C. Creuze, and A. Chemori, "State feedback control of an underwater vehicle for wall following," in *2012 20th Mediterranean Conference on Control & Automation (MED)*, 2012, pp. 542–547.
- [31] M. Prats, J. Prez, J. J. Fernandez, and P. J. Sanz, "An open source tool for simulation and supervision of underwater intervention missions," in *2012 IEEE/RSJ International Conference on Intelligent Robots and Systems*, Oct 2012, pp. 2577–2582.